Accelerated Publications

Light Activation of the LOV Protein Vivid Generates a Rapidly Exchanging Dimer[†,‡]

Brian D. Zoltowski and Brian R. Crane*

Department of Chemistry and Chemical Biology, Cornell University, Ithaca, New York 14853

Received April 21, 2008; Revised Manuscript Received May 21, 2008

ABSTRACT: The fungal photoreceptor Vivid (VVD) plays an important role in the adaptation of blue-light responses in *Neurospora crassa*. VVD, an FAD-binding LOV (light, oxygen, voltage) protein, couples light-induced cysteinyl adduct formation at the flavin ring to conformational changes in the N-terminal cap (Ncap) of the VVD PAS domain. Size-exclusion chromatography (SEC), equilibrium ultracentrifugation, and static and dynamic light scattering show that these conformational changes generate a rapidly exchanging VVD dimer, with an expanded hydrodynamic radius. A three-residue N-terminal β-turn that assumes two different conformations in a crystal structure of a VVD C71V variant is essential for light-state dimerization. Residue substitutions at a critical hinge between the Ncap and PAS core can inhibit or enhance dimerization, whereas a Tyr to Trp substitution at the Ncap−PAS interface stabilizes the light-state dimer. Cross-linking through engineered disulfides indicates that the light-state dimer differs considerably from the dark-state dimer found in VVD crystal structures. These results verify the role of Ncap conformational changes in gating the photic response of *N. crassa* and indicate that LOV−LOV homo- or heterodimerization may be a mechanism for regulating light-activated gene expression.

The Per Arnt Sim (PAS)[1] domain is present in all kingdoms of life as a central component of many signaling pathways where it either mediates protein−protein interactions or acts as a primary sensor. In the latter capacity, a subclass of the PAS domain, the LOV domain (for light, oxygen, voltage) binds a cofactor capable of undergoing chemical changes in response to environmental stimuli (*1*).

LOV domains regulate a diverse set of functions, including nitrogen fixation, gene expression, phototropism, chemotaxis, and the sensing of nitric oxide (*1–7*). Signals propagate from LOV domains in two ways. The LOV domain may affect the activity of an auxiliary domain within the same protein, or the LOV domain may alter its interactions with other partners (*7–12*). The former case is exemplified by the plant phototropins, where two LOV domains (LOV1 and LOV2) regulate the activity of a C-terminal Ser/Thr kinase (*3, 13, 14*). Regulation of kinases by LOV2 domains involves a mechanism where light displaces a C-terminal Jα helix from the LOV2 core (*8, 15, 16*). The LOV1 domain of phototropins undergoes an analogous photocycle to LOV2 but is not required for light-induced activation of kinase activity (*8, 13, 14*). LOV1 stabilizes the phototropin dimer but, unlike LOV2, does not change greatly in conformation following photoexcitation (*14, 17, 18*).

PAS−PAS dimerization is common and extends beyond the phototropins and the LOV family. PAS dimers primarily involve two types of interfaces. The PAS domains of Arnt and hypoxia inducible factor (HIF), KinA histidine kinases, and LOV1-type proteins associate through the PAS β-scaffold (*19–21*). In the case of KinA, the interface appears to be surprisingly versatile, allowing two different association modes for the dimer (*21*). The β-scaffold of the isolated bacterial LOV photoreceptor YtvA also participates in the dimer interface but is assisted by a C-terminal helix (*22, 23*). A second type of PAS−PAS dimer involves a variable N-terminal element external to the core LOV domain called the N-terminal Cap (Ncap) (*10–12*). The heme-based oxygen sensor FixL (*12*), the PAS domain of a soluble guanylyl cyclase from *Nostoc punctiforme* (H-NOXA) (*11*), the nitrogen fixation regulatory protein NifL (*10*), the heme-regulated phosphodiesterase *Ec*DOS (*24*), and CitA form symmetric dimers through N-terminal helices adjacent to the β-scaffold. Ncaps have been suggested to be a universal mode of LOV domain dimerization (*10*); however, despite extensive structural characterization of LOV and PAS dimers,

[†] This work was funded by the National Institutes of Health (Grant GM079679-01).

[‡] Coordinates and structure factors for the Cys71Val variant crystal structure (entry 3D72) have been deposited in the Protein Data Bank.

* To whom correspondence should be addressed: Baker Laboratory, Department of Chemistry and Chemical Biology, Ithaca, NY 14853-1301. Telephone: (607) 255-8634. Fax: (607) 255-1248. E-mail: bc69@cornell.edu.

[1] Abbreviations: VVD, Vivid; LOV, light, oxygen, voltage; Ncap, N-terminal cap; PAS, Per Arnt Sim; SEC, size-exclusion chromatography; HIF, hypoxia inducible factor; WC-1, White Collar 1; WC-2, White Collar 2; WCC, White Collar Complex; MALS, multiangle light scattering; DLS, dynamic light scattering; MW, molecular weight; SAXS, small-angle X-ray scattering; ccgs, clock-controlled genes; wt, wild-type.

10.1021/bi8007017 CCC: $40.75
Published on Web 06/14/2008

their relevance to the full-length proteins is not always clear. For example, full-length YtvA is reported to be monomeric in both the light and dark (*22*). Similarly, the H-NOXA homodimer interface may rather mediate heteroassociations in the full-length protein (*11*). Light-dependent dimerization (and dissociation) of LOV2 domains at millimolar concentrations has also been reported, but again it is unknown if the full-length phototropins have the same properties (*25*).

In the filamentous fungus *Neurospora crassa*, two LOV-domain containing photoreceptors, Vivid (VVD) and White Collar 1 (WC-1), regulate blue-light responses and phase resetting of the circadian clock (*26*). Like the plant phototropins, WC-1 and VVD contain LOV domains that bind FAD as the photosensory element (*5, 26–28*). In addition to the LOV domain, WC-1 contains two other PAS domains, a DNA-binding region, nuclear localization sequences, and transcriptional activation motifs. WC-1 associates with another DNA-binding protein, White Collar 2 (WC-2), to form the White Collar Complex (WCC), which is the primary positive element in the *Neurospora* circadian clock (*26, 29, 30*). VVD, much smaller than WC-1 (a LOV domain with a 70-residue N-terminal extension), participates in light adaptation by antagonizing action of the WCC in response to blue light (*28, 31–33*). Structural, biochemical, and cellular studies implicate a light-induced conformational change in the VVD Ncap that is essential for activity (*34*). However, later steps in the mechanism by which VVD modulates *Neurospora*'s photic response are largely unknown.

The dichotomy between LOV domains that undergo light-stimulated changes in heterooligomerization (i.e., phototropin LOV2) and those that form constitutive LOV−LOV dimers (i.e., NifL and LOV1) may not be that sharp. The presence of an Ncap and the lack of a C-terminal Jα helix place VVD into the LOV1 subclass. However, conformational changes in the VVD Ncap have a strong analogy to light-induced restructuring of the C-termini of phototropin LOV2 domains (*33, 35*). Herein, we report that VVD Ncap conformational changes lead to transient homodimerization, an event that may be key for signal propagation in this LOV subclass.

MATERIALS AND METHODS

Cloning and Protein Expression. N-Terminally truncated VVD constructs were cloned into pet28 (novagen) using the *Nde*I and *Xho*I restriction sites. Point mutations, including A41C, Y50W, M55C, C71V, and E171C, were then introduced into the VVD-36 construct according to the QuickChange protocol (Stratagene). All constructs and mutants were sequenced in their entirety at the Biotechnology Resource Center of Cornell University.

VVD constructs were overexpressed in *Escherichia coli* BL21(DE3) cells. Cultures were induced with 100 μM IPTG at a cell density (OD_{600}) of 0.6−0.8, and proteins were expressed for 22 h at 18 °C under constant light. At all times during purification, VVD proteins were kept in buffers containing 10% glycerol to aid stability. Soluble cell lysate was fractionated by centrifugation and then purified with Ni:NTA affinity chromatography followed by overnight treatment with thrombin. Samples were then purified on a Superdex 75 Hi-load 26/60 FPLC column and concentrated to 4−8 mg/mL.

Size-Exclusion Chromatography. To assay the formation of a light-state dimer, size-exclusion chromatography (SEC) was conducted using a Superdex 75 10/300 analytical column. All samples were injected in 500 μL aliquots with a concentration range of 5−500 μM. The column was equilibrated with buffer containing 50 mM HEPES (pH 8), 150 mM NaCl, and 10% glycerol and run at a flow rate of 0.3 mL/min. Light-state samples were generated by irradiation on ice for 5 min with ambient light sources prior to immediate injection onto the FPLC system. To minimize light exposure during chromatography, the column was covered with aluminum foil during runs with dark-state samples. Approximate dissociation constants were obtained via a fit of total subunit concentration ($[M_F]$) versus the mole fraction monomer (m) and dimer (d) term as shown in eq 1. See the Supporting Information for further discussion regarding this treatment and complications affecting the behavior of VVD on SEC.

$$K_d = \frac{m^2[M_F]}{d(m+2d)} \quad (1)$$

Light Scattering. Both dynamic and static light scattering were used to assay light-state dimerization of VVD proteins. Dynamic light scattering (DLS) was conducted on VVD-36, VVD-44, and VVD C71V with a Protein Solutions Dynapro dynamic light scattering instrument over a concentration range of 5−250 μM. Absolute MW calculations were conducted with a Wyatt miniDAWN Treos multiangle light scattering system. Dark- and light-state samples at 25 μM were injected into a Sephadex 75 10/300 analytical column, which was connected to the Treos. Absolute MW's were determined using ASTRA version 5.0 from Wyatt Technologies. An estimated dissociation constant was obtained with a method analogous to that applied in the SEC treatment. Here, the dissociation constant for each volume slice, v, of 0.05 mL was obtained using eq 1, where the $[M_F]$ was extracted from the absorbance at 280 nm.

The leading edge and trailing edge of the peak yielded slightly different dissociation constants, but because of reduced resolution at the leading edge and some overlap from small amounts of cross-linked dimer, the trailing edge data were taken to be more reliable.

Equilibrium Ultracentrifugation. Equilibrium ultracentrifugation was conducted with a Beckman Coulter Proteomelab XL-1 ultracentrifuge. VVD Y50W at concentrations of 12.5, 25, and 125 μM was subjected to centrifugation at 16000, 20000, and 24000 rpm until successive measurement showed no variation in the concentration profiles. The concentration profiles were measured using absorption measurements at the dark-state maximum (450 nm) and an isosbestic point (413 nm), as well as with interference optics. The 450 nm/413 nm ratio was used to verify the population of the light-state adduct. Concentration profiles were best fit by HeteroAnalysis (*36*) when a single species was assumed.

Crystallography. Monoclinic C71V crystals in space group $P2_1$ were obtained at 22 °C under constant darkness by vapor diffusion. Crystals grew from an equal volume (2 μL) of 6 mg/mL protein dissolved in a buffer containing 50 mM HEPES (pH 8.0), 150 mM NaCl, and 13% glycerol and a reservoir solution containing 100 mM trisodium citrate (pH 5.6), 100 mM ammonium acetate, and 30% PEG 5K MME.

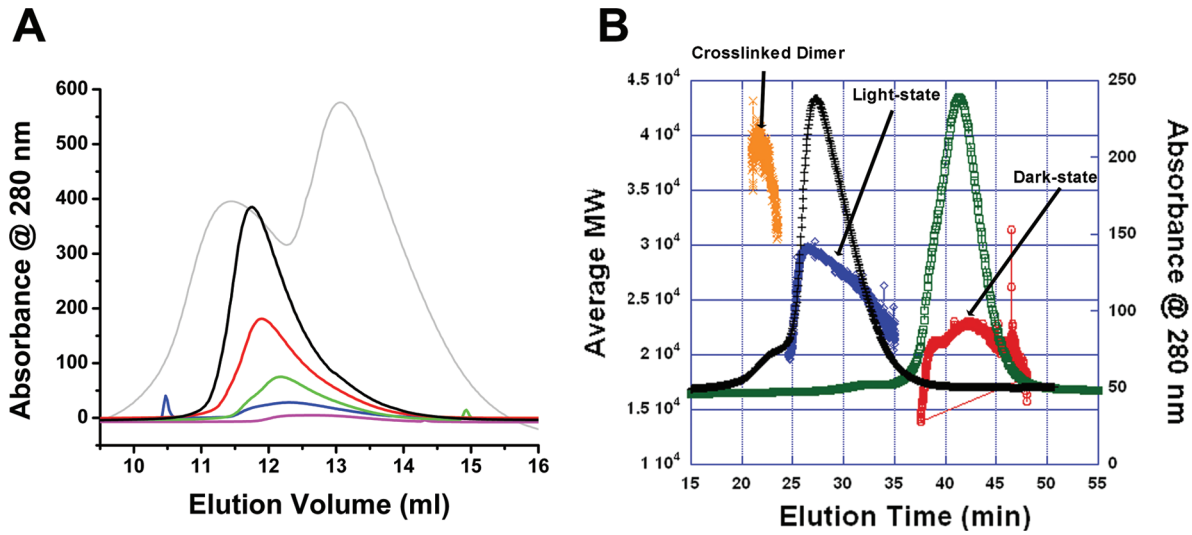

FIGURE 1: (A) Elution profile of VVD-36 at injected concentrations of 150 (black), 75 (red), 30 (green), 15 (blue), and 7.5 μM (magenta). The elution profile for a mixture of cross-linked dimer and dark-state monomer is shown in gray. (B) MALS data with SEC traces for light- and dark-state VVD. The cross-linked dimer reports a molecular mass of 40 kDa (orange). The light state (black SEC trace) increases in molecular mass (blue) as the concentration increases and then decreases on the tail edge of the SEC peak, whereas the dark state (green SEC trace) reports a molecular mass of 20 kDa (red), consistent with a monomer.

VVD C71V crystallizes as single plates, which diffract to ~1.5−1.7 Å resolution. Diffraction data were collected at 100 K on beamline F1 at the Cornell High Energy Synchrotron Source (CHESS). The data were reduced and scaled with HKL2000 (*37*) (Table in the Supporting Information). Initial phases of VVD C71V and the N-terminal structure were obtained by molecular replacement (MR) AmoRe (*38*) using VVD-36 [Protein Data Bank (PDB) entry 2PD7] as a search model. The models were rebuilt using XFIT (*39*), and refinement was conducted with CNS (*40*). Refinement statistics and crystallographic data can be found in the Supporting Information.

RESULTS

The long lifetime of the VVD photoadduct (>10000 s) facilitates study of VVD in both the light- and dark-adapted state (*28*). Furthermore, truncation of the N-terminus by 36 residues generates a more stable protein that maintains the same photocycle as the full-length protein and also undergoes light-induced conformational changes (*34*). Previous work indicated that the hydrodynamic radius of light-state VVD expands relative to that of the dark-state monomer in a manner highly dependent on the length of the N-terminus. In particular, on SEC, the wild type (wt) and the N-terminal variants elute at a single peak with a variable volume that is always intermediate to that of the dark-state monomer and an intentionally cross-linked dimer. Such behavior is consistent with a conformational change in the Ncap that expands the radius of hydration and/or an increase in the time average molecular weight due to formation of a rapidly exchanging equilibrium between monomers and higher oligomers (*34*). In the latter case, the elution volume (v), which reflects both size and shape, should be concentration-dependent, and this was not observed in experiments conducted on a Sephadex 75 26/60 sizing column (Supplementary Figure 1). Attempts to demonstrate dimer formation by pull-down experiments, cross-linking, and spin labeling were unsuccessful (*34*). In addition, small-angle X-ray scattering (SAXS) measurements of the light state indicated expansion of the polypeptide but showed little change in scattering intensity at low angles, which otherwise would reflect oligomerization. Thus, we concluded that the shift in v was due primarily to a structural rearrangement in the Ncap (*34*). However, SEC under different conditions and the properties of newly examined VVD variants have revealed that in addition to Ncap conformational change, the VVD light state will also dimerize to some extent when it is at appropriate concentrations.

Associating systems complicate behavior on SEC. When association affinities are appropriately low and there is fast interconversion between monomers and higher oligomeric states on the time scale of chromatographic separation, samples can elute as a single peak at a position intermediate to that of the pure monomer and the higher oligomer (*41–43*). Although light-state VVD-36 displayed no concentration-dependent shift in small zone SEC on a Superdex 75 26/60 SEC column, its elution profile is concentration-dependent on an analytical Sephadex 75 10/30 column (Supplementary Figure 1 and Figure 1A).[2] Indeed, at high injection concentrations (150 μM), the elution volume matches that of the intentionally cross-linked dimer (Figure 1A), whereas at 7.5 μM, the broad elution profile of the light state approaches that of the dark-state monomer. Similar elution profile shifts are also seen with full-length VVD; however, the instability of the full-length protein prevents a detailed analysis (*34*). All SEC profiles contain a sharp leading edge followed by a long tail, consistent with reacting systems where concentration varies across the peak profile (*41–43*). Under the assumption of a dimeric light state, the concentration dependence of v indicates a K_d in the range of 13 μM.

[2] We do not have a good explanation for why the large SEC column fails to show a concentration dependence for the light-state elution volume. Possibilities may be that in this case, where the sample volume is much smaller than the column volume, equatorial diffusion complicates the elution behavior or that interactions between the sample and the column matrix dominate when there is not a large excess of protein. A more detailed discussion of the complications arising from SEC can be found in the Supporting Information.

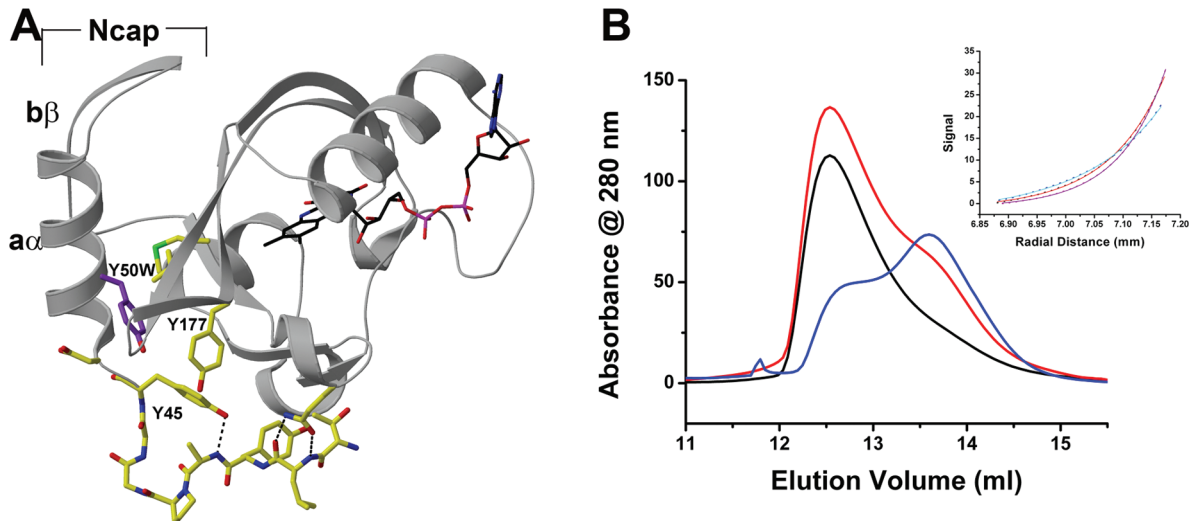

FIGURE 2: Y50 affects dimerization. (A) Structure of the hydrophobic pocket comprised of Y45, Y50 (purple), and Y177. (B) SEC traces of VVD Y50W after light exposure (black) and after darkness for 24 (red) and 48 h (blue). The inset shows equilibrium ultracentrifugation data fit to a single dimeric species (cyan for 16000 rpm, red for 20000 rpm, and magenta for 24000 rpm).

Multiangle light scattering (MALS) was conducted directly following separation of species with SEC to determine the absolute $\overline{MW}$ present in any fractionation volume. MALS of the cross-linked dimer and dark state indicates $\overline{MW}$ values consistent with dimeric (40 kDa) and monomeric (20 kDa) states, respectively (Figure 1B). In contrast, $\overline{MW}$ in the light-state elution peak is concentration-dependent. At the front of the peak, where the concentration is low, VVD is predominantly monomeric. However, as the protein concentration increases, the association equilibrium shifts toward the higher oligomeric state. This causes $\overline{MW}$ to rise to a maximum value and then tail off as the concentration drops on the other side of the elution peak. Notably, even at the highest concentration, $\overline{MW}$ never reaches that of a dimer (Figure 1B) and instead corresponds to a $\overline{MW}$ roughly intermediate between that of the monomer and that of the dimer (~30 kDa). Taking the concentration in each volume slice with the average molar mass given by MALS yields a value for the dissociation constant of 2.6 ± 0.1 μM (Figure 1B). (Although this binding is tighter than that predicted by analysis of ν, the latter suffers from inaccuracies due to column dilution effects that are difficult to quantify.) Furthermore, the VVD light-state elution profiles taken with the column properties provide a lower bound for the dimer dissociation rate constant (k_d) of ~1 s^{-1} (see the Supporting Information). Thus, the somewhat unusual behavior of the VVD light state on SEC arises from relatively rapid dimer dissociation coupled with a sufficiently high association affinity to allow substantial population of the dimeric species.

The VVD dark- and light-adapted states resolved by SEC were characterized by DLS to obtain direct measurements of hydrodynamic radii (R_h) at concentrations where the dimer species dominates. As expected, light-state VVD-36 is significantly expanded (R_h = 3.6 nm) compared to that of the dark state (R_h = 1.9 nm) and the light state of a C71S variant that is biologically inactive (*34*). Although the R_h of 1.9 nm agrees well with that expected for a monomer, a hydrodynamic radius of 3.6 nm indicates a spherical protein of 66 kDa, which is much larger than a VVD-36 dimer (35 kDa). An expanded dimer is consistent with SAXS data that indicate a substantial conformational change in the light state (*34*).

Additional insight into the stoichiometry of the light-state oligomer and the conformational processes involved in its formation were revealed in the properties of a Y50W variant. Y50 lies at the N-terminus of the Ncap helix, and the phenolic side chain packs between the PAS β-sheet and the Ncap where it forms a hydrophobic pocket with Y45, Y177, V168, and M179 (Figure 2A). Spectroscopic analysis of VVD Y50W demonstrates the formation of a stable light-state cysteinyl adduct analogous to native VVD (data not shown). At 4 °C, the recovery of the Y50W variant is very slow (Figure 2B). Despite nearly complete burial of Y50 in the Ncap−PAS core interface, substitution with Trp decreases the dimerization K_d by a factor of 2. The stronger dimer and slow recovery at 4 °C allow analysis of the Y50W light state by analytical equilibrium centrifugation. At equilibrium, the spectroscopically verified light state was nearly completely dimeric (32 kDa) at concentrations from 15 to 150 μM with little evidence of monomer, trimer, or tetramer state (Figure 2B). Thus, the expanded VVD light state as seen by DLS does not likely reflect oligomeric states of an order higher than dimer.

Crystallographic analyses of the VVD light-state crystals revealed a propagation of conformational changes from the flavin active site to the Ncap (*34*). Consistent with these structural changes affecting Ncap structure in solution, SEC of Ncap variants depends highly on N-terminal length. SEC was conducted over a broad concentration range for various N-terminal truncations and extensions of VVD-36. The light states of VVD-22, VVD-30, VVD-38, VVD-40, VVD-42, and VVD-44 all elute as a single species throughout the concentration range that was tested, albeit with a large range of apparent dissociation constants, as given by the concentration dependence of ν (Figure 3). The dissociation properties of the variants fall into three categories depending on the length of the N-terminus: equivalent to VVD-36 K_d (13 ± 1 μM), decreased affinity, and incapable of dimerization. Truncation by six residues (two of which are native residues) of VVD-38 substantially increases the K_d (30 ± 4 μM). Notably, VVD-42 and VVD-44, which remove only four and six additional native residues relative to VVD-38, respectively, do not form any appreciable dimer under all the concentrations that were studied (K_d > 1 mM). DLS of the

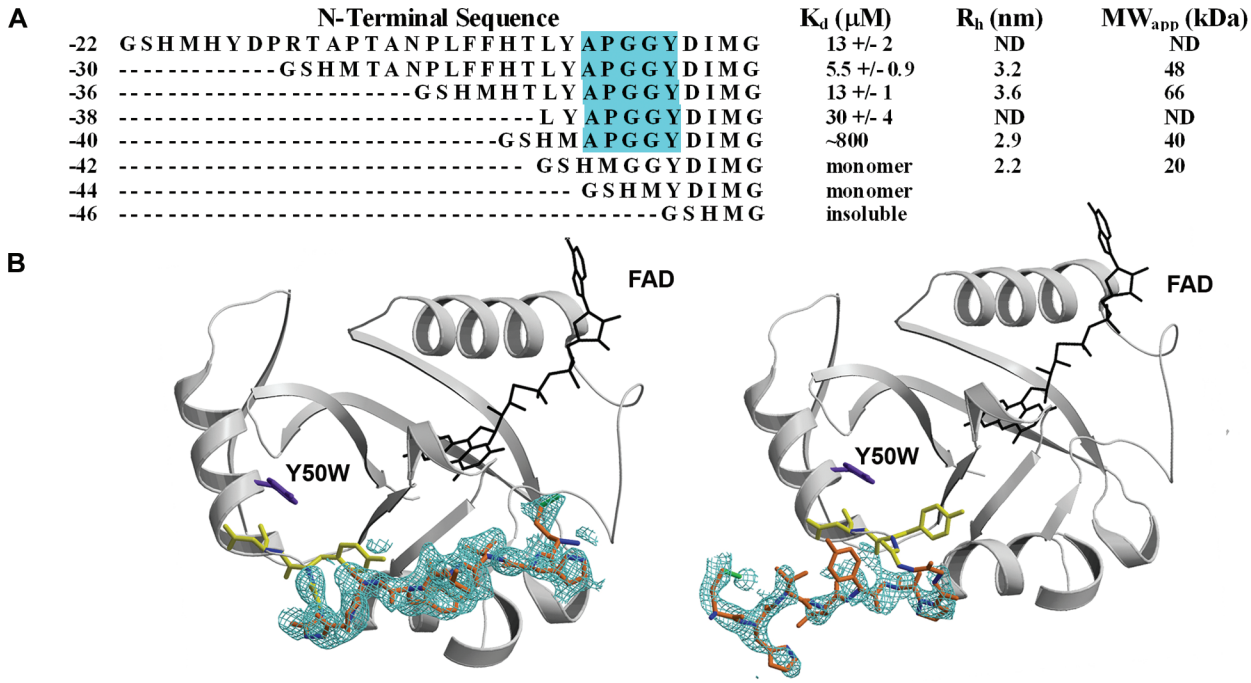

FIGURE 3: (A) Sequence alignment of N-terminal truncations and corresponding dissociation constants. The Pro-Gly-Gly motif that acts as a molecular swivel is highlighted in cyan for the constructs, which undergo light-dependent shifts on SEC. (B) Structure of two conformations of N-terminal residues 37−44 (orange) in different VVD molecules contained within the asymmetric unit of the C71V structure. The $F_o - F_c$ omit map electron density (green) is shown at 2.0σ.

VVD-42 light state gave an R_h of 2.2 nm, which is slightly larger than that of the dark state (1.9 nm) and could reflect conformational change in the light-state monomer. Common to all dimer-forming variants is a Pro-Gly-Gly sequence (Figure 3) at the base of the N-terminal helix. VVD-42 and VVD-38 differ by only the protein sequence LYAP, yet VVD-42 is incapable of forming a dimer. The addition of 6−14 native residues N-terminal to position 36 (VVD-30) had a minimal effect on the dissociation constant (6 and 13 μM, respectively), although R_h decreases in the light state of VVD-30 (3.2 nm) compared to that of VVD-36 [3.6 nm (Figure 3)]. Thus, although residues N-terminal to position 36 may play some role in stabilizing the compact structure of the light state, residues 39−42 are critically important for dimerization. A new 1.65 Å crystal structure of the C71V variant reveals that residues 37−44 can achieve two distinct conformations that vary in their interactions across a crystallographic dimer interface. In previous structures, electron density for residues 37−44 was weak or absent in most molecules in the asymmetric unit. The new structure shows that the two subunits of the crystallographic VVD dimer differ by a 180° rotation about a Pro-Gly-Gly sequence within residues 37−44 (Figure 3). This swivel at Pro42 breaks contacts between the peptide backbone of Leu39 and the Gln80 side chain of the PAS core. Re-examination of previous crystallographic data reveals that this alternate conformation is also occupied in other VVD structures to a small extent (~10−15%). Thus, Pro42 plays a pivotal role in projecting the N-terminus toward the other molecule in the crystallographic dimer.

VVD crystallizes as a symmetric dimer with the Ncap forming the interface. However, cross-linking studies indicate that the crystallographic dimer is unlikely to be the same as the light-state dimer. Cysteine residues introduced at position 55 are well disposed to cross-link the dimer represented in the crystal (Figure 4A). However, upon light excitation, M55C forms virtually no cross-linked dimer. Solvent-exposed Cys residues in the wt sequence and two additional engineered positions also give variable degrees of dark-state cross-linking, but no significant increase in cross-linking upon light exposure (Figure 4A,B). In contrast, light enhances cross-linking of the E171C variant, despite these positions being held 23.6 Å apart by the Ncaps that construct the dimer interface in the crystal (Figure 4A,B). Surprisingly, SEC indicates that VVD cross-linked at residue 171 will still recruit additional molecules to the disulfide-linked dimer upon light excitation (Supplementary Figure 2). Thus, position 171 must be close to the light-state dimer interface, but not directly in it; otherwise, cross-linking at this position would prevent further oligomerization.

Crystallographic studies of the light state show how changes in the VVD Ncap are gated by conformational perturbations that propagate from the flavin ring through the hinge connecting the Ncap to the PAS core (*34*). Q182 alters hydrogen-bonding partners due to protonation of the flavin ring at N5 in the cysteinyl adduct state. This correlates with movement of the C71 side chain from a buried position to one where it interacts with bβ. A C71S substitution that cannot undergo this change in conformation was inactive both in vitro and in vivo (*34*). In contrast, a C71V variant underwent normal conformational changes in vitro (*34*). VVD C71V elutes as a single species by SEC under all concentrations that were tested (Figure 4C). However, C71V has a substantially lower dissociation constant for dimer formation than the wt sequence (0.4 vs 13 μM by SEC). The crystal structure of this variant reveals that one of the Val side chain methyl groups resides at the position occupied by the C71 thiol in the dark state and the other side chain methyl mimics the C71 thiol in the light state (Figure 4D). Thus, the position of the Val side chain predisposes the VVD

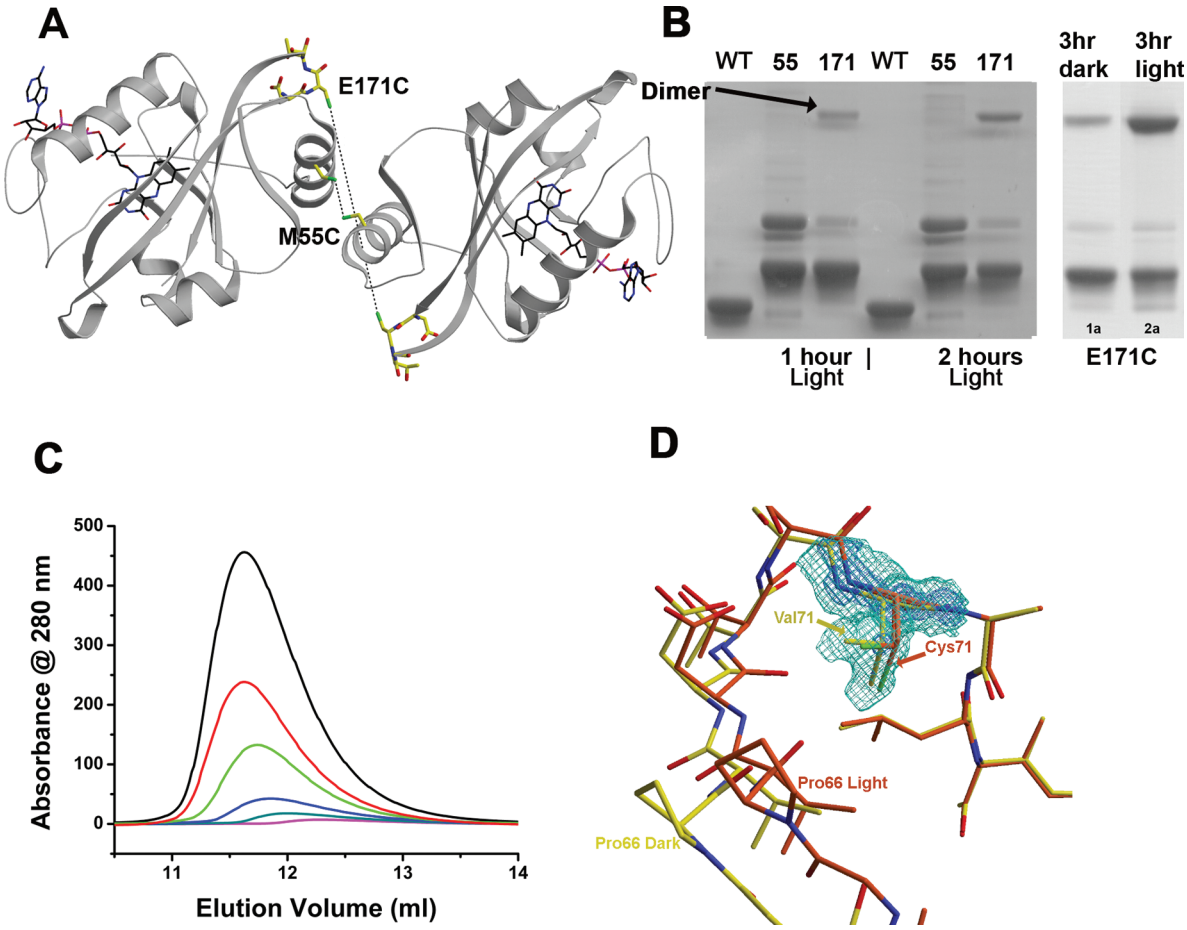

FIGURE 4: Light-state dimer and crystallographic dimer differ. (A) M55C is buried in the dimer interface but does not cross-link, whereas E171C is separated by 23.6 Å and cross-links readily. (B) SDS−PAGE indicates that VVD-36 and M55C do not cross-link in the dark or light, but E171C cross-links readily after light exposure in a time-dependent manner. HIS_6-tags are retained in the mutants. (C) C71V produces a more stable light-state dimer. Elution profile of VVD-36 C71V at injected concentrations of 150 (black), 75 (red), 30 (green), 15 (blue), and 7.5 μM (magenta). (D) Val71 in the C71V variant simultaneously fills positions held by the native Cys71 thiol in both the dark and light states.

Ncap toward the light-state conformation, thereby facilitating dimer formation. The combined data disclose a light-state dimerization driven by conformational changes at two key regions: (1) the Ncap Pro-Gly-Gly sequence and (2) the hinge to the PAS core (Figure 4D).

DISCUSSION

These studies yield a picture of VVD light activation in which the flavin protonation state is read out by a series of compensating conformational and hydrogen bonding changes that lead through Q182 and C71 to the Ncap, where restructuring produces a new interface for dimerization. For a number of reasons, the VVD light-state dimer must differ from the VVD dimer represented in crystals of the dark state. Light inhibits crystallization, and the symmetric contacts between aα, as found in the dark-state crystal structure, could not be cross-linked through Cys substitutions; position 171 readily cross-links even though it should be held apart by the crystallographic dimer. Furthermore, the behaviors of the C71S, C71V, Y50W, and Ncap variants indicate that the interface between the Ncap and the PAS β-scaffold changes during light-induced dimerization. Complete removal of the Ncap prevents expression of the recombinant protein in *E. coli*, as do some point mutations in the interface between the Ncap and the β-sheet (*34*). N-Terminal residues 38−42 are essential for light-induced dimerization, and some residue substitutions on aα also prevent assembly (e.g., I52R). However, we do not know if these sites stabilize a subunit conformation conducive to association or if they participate directly in the dimer interface. The surface-exposed FAD adenosine moiety is also unlikely to participate in the dimer interface, as its removal by phosphodiesterase treatment does not prevent the change in hydrodynamic radius (*34*). Residues 39−42 are essential for dimerization and can swivel about a conserved Pro-Gly-Gly motif. The mobility of the N-terminus appears to contribute to the expanded state of VVD-36 (R_h = 3.6 nm), as addition of six residues to VVD-30 (R_h = 3.2 nm) decreases the size of the light-state dimer while increasing the dimer affinity (13 and 5.5 μM, respectively). Repacking of the aα helix against the PAS core leading to full or partial release of the N-terminus would be consistent with the mutational data and expanded monomeric state suggested by SAXS and DLS. Once released, the N-terminus may then provide new interactions with the adjacent subunit in the rapidly exchanging dimer. In fact, dimerization of H-NOXA is also highly sensitive to the length of the N-terminus (*11*). In the H-NOXA crystal structure, residues N-terminal to the Ncap helix swap to contact the adjacent subunit in the dimer. If VVD dimerization involves a similar domain swapping process, it must

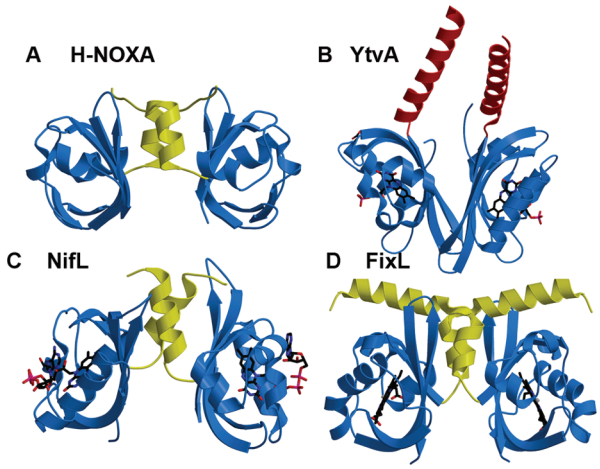

FIGURE 5: Structures representative of PAS dimers H-NOXA (A), YtvA (B), NifL (C), and FixL (D). The Ncaps (yellow) of panels A, C, and D form a similar dimer interface, whereas the C-terminal extension of D (red) and the PAS core (blue) associate the subunits.

allow motion of the 36 N-terminal residues not present in our structures. FixL and NifL also form constitutive Ncap-mediated dimers (Figure 5) and are not known to undergo a regulated switch in oligomeric state (*10–12*). The LOV domain from the bacterial photosensor YtvA forms a different constitutive dimer with an interface composed of the PAS β-scaffold and C-terminal helices, the latter of which project toward the signaling domain (*10–12, 22, 23*). The alternative conformations of the VVD Pro-Gly-Gly sequence suggest that the light-state dimer shares similarities with the domain-swapped Ncap contacts of HNOX-A. On the other hand, the cross-linking experiments suggest that a β-sheet$-\beta$-sheet contact, similar to that of YtvA, may be accessed after partial or complete dissociation of the Ncap. The degree to which the very different HNOX-A or YtvA constitutive dimers are related to the VVD light-state dimer remains to be determined.

Blue-Light Signaling in N. crassa. Blue-light photoregulation of gene expression is a two-step process in *Neurospora* that involves LOV domains from both WC1 and VVD. WC-1 associates with WC-2 on various promoters to form the WCC, a transcriptional activator. Following blue-light exposure, WC-1 is also converted to a cysteinyl C4a flavin adduct. A WC-1 chimera, in which the WC-1 LOV domain has been replaced with that of VVD, retains blue-light-induced responses in *Neurospora*, indicative of a common mechanism (*2*). Moreover, gel shift assays indicate that the size or conformation of the WCC on DNA alters upon light activation in a manner that may indicate LOV$-$LOV dimerization analogous to that observed for VVD (*5*). The WCC then induces the expression of clock-controlled genes (ccgs), which include *vvd* (*5, 26, 32, 44*). VVD accumulates and allows for a secondary photic response (*32*). Newly produced VVD antagonizes transcriptional activation by the WCC and regulates phosphorylation of WC-1 (*5, 26, 32, 44*). Given the sequence similarity and related properties of VVD and WC-1, it is tempting to speculate that light-activated VVD may compete for binding to the WC-1 LOV domain, disrupting light-activated WC-1 homodimerization and thereby inhibiting gene expression. A dissociation constant commensurate with that measured for VVD-36 ($2-10\ \mu$M) may be relevant in the environment of the ccg promoter where the LOV domain has a high effective concentration. However, it must be noted that there are currently no data demonstrating interactions among VVD, WC-1, and WC-2 and some evidence that VVD is primarily localized to the cytoplasm (*28*). Thus, the primary target of the VVD light-state monomer may be an entirely different partner that can bind the remodeled recognition surface and then convey signals to the WCC. In either scenario, coupling light-induced conformational states to oligomerization equilibria extends the original light signal in time and amplifies it in spatial extent. The discovery of VVD variants such as Y50W and C71V that stabilize the signaling state may facilitate the discovery of VVD's targets.

ACKNOWLEDGMENT

We thank Wyatt Technologies and Qian Yin and Hao Wu at the Weill Cornell Medical Center for assistance with MALS. We also thank Jennifer Loros and Jay C. Dunlap for helpful discussions.

SUPPORTING INFORMATION AVAILABLE

Discussion on SEC determination of dissociation constants, a table of crystallographic data, non-concentration-dependent behavior on a preparative sizing column (Supplementary Figure 1), SEC concentration-dependent shift for E171C (Supplementary Figure 2), and dark-state elution profiles for VVD-30, VVD-38, and VVD-42 (Supplementary Figure 3). This material is available free of charge via the Internet at http://pubs.acs.org.

NOTE ADDED AFTER ASAP PUBLICATION

This paper was published ASAP on June 14, 2008 with errors in the Results section. The correct version was published on July 1, 2008.

REFERENCES

1. Crosson, S., Rajagopal, S., and Moffat, K. (2003) The LOV Domain Family: Photoresponsive Signaling Modules Coupled to Diverse Output Domains. *Biochemistry 42*, 2–10.
2. Cheng, P., He, Q., Yang, Y., Wang, L., and Liu, Y. (2003) Functional conservation of light, oxygen, or voltage domains in light sensing. *Proc. Natl. Acad. Sci. U.S.A. 100*, 5939–5943.
3. Christie, J. M. (2007) Phototropin Blue-Light Receptors. *Annu. Rev. Plant Biol. 58*, 21–45.
4. Dixon, R. (1998) The oxygen-responsive NIFL-NIFA complex: A novel two-component regulatory system controlling nitrogenase synthesis in γ-Proteobacteria. *Arch. Microbiol. 169*, 371–380.
5. Froehlich, A., Liu, Y., Loros, J. J., and Dunlap, J. C. (2002) White Collar-1, a Circadian Blue Light Photoreceptor, Binding to the frequency Promoter. *Science 297*, 817–819.
6. Schmoll, M., Franchi, L., and Kubicek, C. P. (2005) Envoy, A PAS/LOV Domain Protein of *Hypocrea jecorina* (Anamorph *Trichoderma reesei*), Modulates Cellulase Gene Transcription in Response to Light. *Eukaryotic Cell 4*, 1998–2007.
7. Taylor, B., and Zhulin, I. B. (1999) PAS Domains: Internal Sensors of Oxygen, Redox Potential, and Light. *Microbiol. Mol. Biol. Rev. 63*, 479–506.
8. Harper, S. M., Christie, J. M., and Gardner, K. H. (2004) Disruption of the LOV-Jα Helix Interaction Activates Phototropin Kinase Activity. *Biochemistry 43*, 16184–16192.
9. Taylor, B. L., and Zhulin, I. B. (1998) In search of higher energy: Metabolism-dependent behaviour in bacteria. *Mol. Microbiol. 28*, 683–690.
10. Key, J., Hefti, M., Purcell, E. B., and Moffat, K. (2007) Structure of the Redox Sensor Domain of *Azotobacter vinelandii* NifL at Atomic Resolution: Signaling, Dimerization and Mechanism. *Biochemistry 46*, 3614–3623.

11. Ma, X., Sayed, N., Baskaran, P., Beuve, A., and ban den Akker, F. (2007) PAS-mediated Dimerization of Soluble Guanylyl Cyclase Revealed by Signal Transduction Histidine Kinase Domain Crystal Structure. *J. Biol. Chem. 283*, 1167–1178.
12. Miyatake, H., Mukai, M., Park, S. Y., Adachi, S., Tamura, K., Nakamura, H., Nakamura, K., Tsuchiya, T., Lizuka, T., and Shiro, Y. (2000) Sensory Mechanism of Oxygen Sensor FixL from *Rhizobium meliloti*: Crystallographic, Mutagenesis and Resonance Raman Spectroscopic Studies. *J. Mol. Biol. 301*, 415–431.
13. Christie, J. M., Swartz, T. E., Bogomolni, R. A., and Briggs, W. R. (2002) Phototropin LOV domains exhibit distinct roles in regulating photoreceptor function. *Plant J. 32*, 205–219.
14. Matsuoka, D., and Tokutomi, S. (2005) Blue light-regulated molecular switch of Ser/Thr kinase in photoropin. *Proc. Natl. Acad. Sci. U.S.A. 102*, 13337–13342.
15. Eitoku, T., Nakasone, Y., Matsuoka, D., Tokutomi, S., and Terazima, M. (2005) Conformational dynamics of phototropin 2 LOV2 domain with the linker upon photoexcitation. *J. Am. Chem. Soc. 127*, 13238–13244.
16. Harper, S. M., Neil, L. C., and Gardner, K. H. (2003) Structural Basis of a Phototropin Light Switch. *Science 301*, 1541–1544.
17. Nakasako, M., Iwata, T., Matsuoka, D., and Tokutomi, S. (2004) Light-induced structural changes of LOV domain-containing polypeptides from *Arabidopsis* phototropin 1 and 2 studied by small-angle X-ray scattering. *Biochemistry 43*, 14881–14890.
18. Salomon, M., Lempert, U., and Rudiger, W. (2004) Dimerization of the plant photoreceptor phototropin is probably mediated by the LOV1 domain. *FEBS Lett. 572*, 8–10.
19. Card, P. B., Erbel, P. J. A., and Gardner, K. H. (2005) Structural Basis of ARNT PAS-B Dimerization: Use of a Common β-sheet Interface for Hetero- and Homodimerization. *J. Mol. Biol. 353*, 664–667.
20. Erbel, P. J. A., Card, P. B., Karakuzu, O., Bruick, R. K., and Gardner, K. H. (2003) Structural basis for PAS domain heterodimerization in the basic helix-loop-helix PAS transcription factor hypoxia-inducible factor. *J. Mol. Biol. 100*, 15504–15509.
21. Lee, J., Tomchick, D. R., Brautigam, C. A., Machius, M., Kort, R., Hellingwerf, K. J., and Gardner, K. H. (2008) Changes at the KinA PAS-A Dimerization Interface Influence Histidine Kinase Function. *Biochemistry 47*, 4051–4064.
22. Buttani, V., Losi, A., Eggert, T., Krauss, U., Jaeger, K.-E., Cao, Z., and Gartner, W. (2007) Conformational analysis of the blue-light sensing protein YtvA reveals a competitive interface for LOV-LOV dimerization and interdomain interactions. *Photochem. Photobiol. Sci. 6*, 41–49.
23. Moglich, A., and Moffat, K. (2007) Structural Basis for Light-dependent Signalling in the Dimeric LOV Domain of the Photosensor YtvA. *J. Mol. Biol. 373*, 112–126.
24. Kurokawa, H., Lee, D.-S., Watanabe, M., Sagami, I., Mikami, B., Raman, C. S., and Shimizu, T. (2004) A Redox-controlled Molecular Switch Revealed by the Crystal Structure of a Bacterial Heme PAS Sensor. *J. Biol. Chem. 279*, 20186–20193.
25. Nakasone, Y., Eitoku, T., Matsuoka, D., Tokutomi, S., and Terazima, M. (2006) Kinetic Measurement of Transient Dimerization and Dissociation Reactions of *Arabidopsis* Phototropin 1 LOV2 Domain. *Biophys. J. 91*, 645–653.
26. Loros, J. J., and Dunlap, J. C. (2001) Genetic and Molecular Analysis of Circadian Rhythms in Neurospora. *Annu. Rev. Physiol. 63*, 757–794.
27. He, Q., Cheng, P., Yang, Y., Wang, L., Gardner, K. H., and Liu, Y. (2002) White Collar-1, a DNA Binding Transcription Factor and a Light Sensor. *Science 297*, 840–843.
28. Schwerdtfeger, C., and Linden, H. (2003) VIVID is a flavoprotein and serves as a fungal blue light photoreceptor for photoadaptation. *EMBO J. 22*, 4846–4855.
29. Lee, K., Dunlap, J. C., and Loros, J. J. (2003) Roles for WHITE COLLAR-1 in Circadian and General Photoreception in *Neurospora crassa*. *Genetics 163*, 103–114.
30. Lee, K., Loros, J. J., and Dunlap, J. C. (2000) Interconnected Feedback Loops in the *Neurospora* Circadian System. *Science 289*, 107.
31. Elvin, M., Loros, J. J., Dunlap, J. C., and Heintzen, C. (2005) The PAS/LOV protein VVD supports a rapidly dampened daytime oscillator that facilitates entrainment of the *Neurospora* circadian clock. *Genes Dev. 19*, 2593–2605.
32. Heintzen, C., Loros, J. J., and Dunlap, J. C. (2001) The PAS Protein VIVID Defines a Clock-Associated Feedback Loop that Represses Light Input, Modulates Gating, and Regulates Clock Resetting. *Cell 104*, 453–464.
33. Shrode, L. B., Lewis, Z. A., White, L. D., Bell-Pedersen, D., and Ebbole, D. J. (2001) vvd Is Required for Light Adaptation of Conidiation-Specific Genes of *Neurospora crassa*, but Not Circadian Conidiation. *Fungal Genet. Biol. 32*, 169–181.
34. Zoltowski, B. D., Schwerdtfeger, C., Widom, J., Loros, J. J., Bilwes, A. M., and Crane, B. R. (2007) Conformational Switching in the Fungal Light Sensor Vivid. *Science 316*, 1054–1057.
35. Ko, W.-H., Nash, A. I., and Gardner, K. H. (2007) A LOVely view of blue light photosensing. *Nat. Chem. Biol. 3*, 372–374.
36. Cole, J. L. (2004) Analysis of Heterologous Interactions. *Methods Enzymol. 384*, 212–232.
37. Otwinowski, A., and Minor, W. (1997) Processing of X-ray diffraction data in oscillation mode. *Methods Enzymol. 276*, 307–325.
38. Navaza, J. (1994) AMoRe: An automated package for molecular replacement. *Acta Crystallogr. A50*, 157–163.
39. McRee, D. E. (1992) XtalView: A visual protein crystallographic software system for X11/Xview. *J. Mol. Graphics 10*, 44–47.
40. Brunger, A. T., Adams, P. D., Clore, G. M., Delano, W. L., Gros, P., Grosse-Kunstleve, R. W., Jiang, J. S., Kuszewski, J., Nilges, M., Pannu, N. S., Read, R. J., Rice, L. M., Simonson, T., and Warren, G. L. (1998) Crystallography and NMR system: A new software suite for macromolecular structure determination. *Acta Crystallogr. D54*, 905–921.
41. Ackers, G. K. (1975) Molecular sieve methods of analysis. In *The Proteins* (Neurath, H., and Hill, R. L., Eds.) pp 1−94, Academic Press, New York.
42. Stevens, F. J. (1989) Analysis of protein-protein interaction by simulation of small-zone size exclusion chromatography. *Biophys. J. 55*, 1155–1167.
43. Winzor, D. J., and Scheraga, H. A. (1963) Studies of Chemically Reacting Systems on Sephadex I. Chromatographic Demonstration of the Gilbert Theory. *Biochemistry 2*, 1263–1267.
44. Froehlich, A. C., Loros, J. J., and Dunlap, J. C. (2003) Rhythmic binding of a White Collar-containing complex to the frequency promoter is inhibited by frequency. *Proc. Natl. Acad. Sci. U.S.A. 100*, 5914–5919.

BI8007017